ELSEVIER

Chemical Engineering Journal 133 (2007) 257–264

Chemical Engineering Journal

www.elsevier.com/locate/cej

Mass transfer characteristics of a novel multi-stage external loop airlift reactor

Kaustubha Mohanty [a,*], Debabrata Das [b], Manindra Nath Biswas [a]

[a] *Department of Chemical Engineering, Indian Institute of Technology, Kharagpur 721 302, India*
[b] *Department of Biotechnology, Indian Institute of Technology, Kharagpur 721 302, India*

Received 6 June 2006; received in revised form 26 September 2006; accepted 14 February 2007

Abstract

This paper reports on the experimental investigation carried out to evaluate the interfacial area, a, and liquid-side volumetric mass transfer coefficient, $k_L a$, to characterize a multi-stage external loop airlift reactor (with contraction and expansion disks), which has been conceived, designed, and fabricated as an equipment to remove trace pollutants from wastewater. In addition, it has versatile use as a gas–liquid contactor in chemical process industries. In the experimental range of gas and liquid flows investigated, the maximum interfacial area and volumetric mass transfer coefficient obtained was in the order of 300 m^2/m^3 and 0.05 s^{-1}, respectively. Correlations developed for predicting the interfacial area and liquid-side volumetric mass transfer coefficient have been found to be encouraging and highly significant from statistical analysis.

Keywords: Multi-stage reactor; External loop airlift reactor; Interfacial area; Volumetric mass transfer coefficient

1. Introduction

External loop airlift reactors (ELALRs) have drawn much attention due to their simple construction, good heat and mass transfer, and good mixing characteristics as the gas phase serves the dual functions of aeration and agitation [1–3]. The special feature distinguishing ELALRs from conventional bubble columns is the recirculation of the liquid through an external downcomer that connects the gas–liquid separator and the bottom of the riser. The density difference between the gas and the liquid passing through the riser induces circulation of the liquid in the ELALR. The circulation creates good mixing in all phases and provides good mass transfer. In addition the external loop facilitates temperature control in the reactor [3].

However, a simple ELALR operates in one stage only, and therefore high efficiency cannot be achieved. To achieve a high efficiency of mass transfer, ELALRs must be operated either in series or in multiple stages because of the limitations of a specific interfacial area, a and the mass transfer coefficient, $k_L a$ in a single stage ELALR. In some earlier works, mainly with bubble columns, different internals like baffles, plates and screens were used to increase the efficiency, which resulted in high energy dissipation and complex mechanical construction leading to difficulty in operation [4–8]. To overcome these drawbacks, a variable-area multi-stage external loop airlift reactor has been designed, fabricated and characterized.

In the present investigation, an ELALR, operating in three stages, has been designed. The staging effect of the present reactor has been achieved through hydrodynamically induced continuous bubble generation, break-up and regeneration. The presence of rupture and expansion disks helps to generate finer dispersion, which in turn increases the fractional gas holdup of the system. Large gas holdup favors improved mass transfer, which is essential for an efficient equipment treating wastewater. The system has been made to operate with relatively large sized bubbles and minimum hydrodynamic cavitation, so that internal circulation can be induced in the liquid–bubble interfaces and faster transfer of components can take place both by turbulent diffusion through the interface of the bubbles and also due to the direct rupture of the relatively large sized bubbles [8].

A review of literature reveals that considerable work has been carried out on the measurement of the interfacial area and volumetric mass transfer coefficient by light attenuation, high-speed photography, and chemical method. These methods were described in detail elsewhere [9–13].

* Corresponding author. Tel.: +91 3222 282249; fax: +91 3222 282250.
E-mail addresses: kmohanty@che.iitkgp.ernet.in, mohanty_k_iit@yahoo.com (K. Mohanty).

1385-8947/$ – see front matter © 2007 Elsevier B.V. All rights reserved.
doi:10.1016/j.cej.2007.02.007

Nomenclature

a	specific interfacial area per unit volume (m^2/m^3)
C_A^*	concentration of dissolved gas at the interface, in equilibrium with gas at the interface ($kg\,mol/m^3$)
C_B^o	concentration of reactant B in the bulk of the solution ($kg\,mol/m^3$)
D_A	diffusivity of dissolved gas A (m^2/s)
G	molar flowrate of the reacting diluent gas (g mol/s)
G'	molar flowrate of inert gas (g mol/s)
h	sum of contribution of ions to solubility factors (L/g mol)
He	Henry's law constant (cm^3 atm/g mol)
I	ionic strength (g ion/L)
k_L	liquid-side mass transfer coefficient (m/s)
k_{LR}	coefficient of chemical absorption $(D_A k_2 C_B^o)^{1/2}$ (cm/s)
k_2	second order reaction rate constant (cm^3/g mol s)
K_W	ionic product of water $(g\,mol/L)^2$
K_2	equilibrium values of $[H^+][CO_3^{2-}]/[HCO_3^-]$ (g mol/L)
p_A	partial pressure of A (atm)
p_A^*	equilibrium partial pressure of A (atm)
P'	system pressure (atm)
R_a	rate of absorption per unit area ($kg\,mol/m^3$ s)
T	temperature (K)
U_G	superficial liquid velocity (m/s)
U_L	superficial liquid velocity (m/s)
U_{LC}	liquid circulation velocity (m/s)
V	volume of gas–liquid mixture inside the column (m^3)
V_L	volume of liquid inside the column (m^3)
y	composition of CO_2 in gas phase (mol%)
y_i	composition of CO_2 in gas phase at outlet (mol%)
y_o	composition of CO_2 in gas phase at inlet (mol%)

Greek letter

ε_G	fractional gas holdup

Subscripts

−	anion
+	cation
B	used for liquid
G	gas
I	ionization

Because in the present system the intense mixing between phases generates high turbulence, the first two methods were considered unsuitable and, therefore, the chemical method was selected. This paper presents a detailed experimental investigation of the measurement of the interfacial area and volumetric mass transfer coefficient by the chemical method of absorbing CO_2 in sodium hydroxide and sodium carbonate/bicarbonate buffer solution. Correlations for predicting the interfacial area and volumetric mass transfer coefficient in terms of superficial gas velocity have been developed.

2. Theoretical consideration

Brian [14] has discussed the theory of absorption followed by a chemical reaction of the general order. The liquid phase reaction between dissolved carbon dioxide and sodium hydroxide satisfies the condition for pseudo-first order reaction at certain alkali concentration, and was therefore selected for the present study. This reaction is said to take place as:

$$CO_2 + OH^- \rightarrow HCO_3^- \quad (1)$$

$$HCO_3^- + OH^- \rightarrow CO_3^{2-} + H_2O \quad (2)$$

Since the second reaction is ionic, it takes place at a much faster rate than the first one, therefore, the first reaction step is rate controlling. The second order rate constant, k_2, was determined by the equation suggested by Porter et al. [15]:

$$\log_{10} k_2 = 16.635 - \frac{2895}{T} + 0.132I \quad (3)$$

If the concentration of OH^- remains essentially constant in the bulk of the solution, the equation becomes pseudo-first order. The condition to be satisfied for this is given by the following condition as suggested by Danckwerts [16]:

$$\left[\frac{D_A k_2 C_B^o}{k_L^2}\right]^{1/2} \ll 1 + \frac{C_B^o}{2C_A^*} \quad (4)$$

D_A, the diffusivity of carbon dioxide in aqueous solutions was obtained by the equation reported by Nijsing et al. [17]. It has been shown by Sharma and Danckwerts [12] that the specific rate of absorption per unit area for a second order reaction satisfying the condition of Eq. (4) is:

$$R_a = C_A^* \sqrt{D_A k_2 C_B^o + k_L^2} \quad (5)$$

$$\text{If further,} \quad \left[\frac{D_A k_2 C_B^o}{k_L^2}\right]^{1/2} > 3 \quad (6)$$

the second term within the square root of Eq. (5) becomes small compare to the first term and, therefore, the specific rate is given by the simplified equation:

$$R_a = C_A^* \sqrt{D_A k_2 C_B^o} = C_A^* k_{LR} \quad (7)$$

When the condition given by Eqs. (4) and (6) are satisfied, the rate of absorption will be a function of the physico-chemical factors and will be independent of the hydrodynamic conditions in the system. If further the gas phase resistance can be neglected, the concentration of carbon dioxide at the inter-phase, C_A^*, is related to its partial pressure in the gas phase by:

$$p_A^* = \mathrm{He} C_A^* = p_A = yP' \quad (8)$$

where He is the Henry's law constant in the solution and obtained by means of the following expression:

$$\log_{10}\left(\frac{\mathrm{He}}{\mathrm{He^o}}\right) = hI \tag{9}$$

where $\mathrm{He^o}$ is the value in water, I the ionic strength of the solution and h is the solubility parameter available in literature [16]. There are some experimental evidences in literature [15] to suggest that gas phase resistance does not exceed about 10% of total resistance and can be neglected. Therefore, following the method suggested by Voyer and Miller [18] and assuming plug flow in the gas phase and perfect mixing in the liquid phase, one can write, the rate of absorption in a differential volume dv:

$$R_\mathrm{a}\,\mathrm{d}v = aC_\mathrm{A}^* k_\mathrm{LR}\,\mathrm{d}v \tag{10}$$

From a material balance equation on a solute free basis, we have:

$$G' = G(1-y) \tag{11}$$

Therefore, rate of absorption in a differential volume dv:

$$-\mathrm{d}(Gy) = -\mathrm{d}\left(\frac{G'y}{1-y}\right) = -\frac{G'\,\mathrm{d}y}{(1-y)^2} \tag{12}$$

From Eqs. (10) and (12) we obtain:

$$aC_\mathrm{A}^* k_\mathrm{LR}\,\mathrm{d}v = -\frac{G'\,\mathrm{d}y}{(1-y)^2} \tag{13}$$

Substituting the value of C_A^* from Eq. (8) we get:

$$\frac{ak_\mathrm{LR}yP'}{\mathrm{He}}\mathrm{d}v = -\frac{G'\,\mathrm{d}y}{(1-y)^2} \tag{14}$$

$$\text{therefore,}\quad \frac{ak_\mathrm{LR}P'}{G'\,\mathrm{He}}\mathrm{d}v = -\frac{\mathrm{d}y}{y(1-y)^2} \tag{15}$$

Integrating Eq. (15) over the total system volume and rearranging the following expression for interfacial area can be obtained:

$$a = \frac{G'\,\mathrm{He}}{k_\mathrm{LR}P'V}\ln\left[\frac{1-y_\mathrm{o}}{y_\mathrm{o}}\frac{y_\mathrm{i}}{1-y_\mathrm{i}}\right] + \left[\frac{1}{1-y_\mathrm{i}} - \frac{1}{1-y_\mathrm{o}}\right] \tag{16}$$

Eq. (16) can be used to determine the specific interfacial area, provided the conditions for the pseudo-first order reaction and fast reaction are satisfied.

A diffusion controlled slow reaction is suitable for determining the liquid volumetric mass transfer coefficient, $k_\mathrm{L}a$. The absorption of CO_2 into a carbonate–bicarbonate buffer solution is a convenient system, and is represented by Eq. (1). Under certain condition the above reaction is sufficiently fast, so that the concentrations of CO_2 in the bulk of the liquid phase close to zero. The condition to be satisfied for this is:

$$k_\mathrm{L}a \ll \alpha_\mathrm{L}k_2C_\mathrm{B}^\mathrm{o} \tag{17}$$

Further, the reaction rate is such that no appreciable amount of reaction takes place in the diffusion films, and the condition to be satisfied for this is given by:

$$\frac{D_\mathrm{A}k_2C_\mathrm{B}^\mathrm{o}}{k_\mathrm{L}^2} \ll 1 \tag{18}$$

The concentration of hydroxyl ion in a carbonate–bicarbonate mixture was obtained by the following expression:

$$C_\mathrm{B}^\mathrm{o} = \frac{K_\mathrm{W}}{K_2}\frac{[{CO_3}^{2-}]}{[{HCO_3}^{-}]} \tag{19}$$

The variation of K_2 with temperature was given by Harned and Owen [19] and can be written as:

$$\log K_2 = -\frac{2902.4}{T} + 6.498 - 0.0238T \tag{20}$$

When the condition given by Eqs. (17) and (18) are satisfied, the rate of mass transfer is given by:

$$R_\mathrm{a} = k_\mathrm{L}aC_\mathrm{A}^* \tag{21}$$

By measuring, R_a, the rate of mass transfer per unit volume, the rate of volumetric coefficient, $k_\mathrm{L}a$, can be determined from Eq. (21).

3. Experimental setup and techniques

The schematic diagram of the experimental setup is shown in Fig. 1. The experimental column has been constructed in three vertical stages, which in effect operate in series. The reactor consists of a vertical cylindrical perspex column of 0.2199 m diameter and 1.82 m long, fitted onto a fructo-conical bottom made up of perspex. The latter had a divergence angle of 7° and a height of 0.76 m. The minimum diameter of the fructo-conical section was 0.1 m. The vertical cylindrical column was fitted with a total of seven internals (four contraction disks and three expansion disks). The contraction and expansion disks had central axial openings of 0.1099 and 0.00635 m (size of a single opening on the screen of diameter 0.2199 m), respectively. All the contraction and expansion disks were placed at equal distances from each other and were supported on the column by means of threaded screws. At the bottom most section of the cylindrical column, just above the fructo-conical cone, was fitted an antenna type of sparger for generating bubbles uniformly throughout the entire cross-section of the column.

At the bottom of the first or lowest stage of the reactor, a swarm of bubbles are generated at relatively high velocities with the help of a multi-orifice sparger. At the beginning of the first stage bubbles have been ruptured and coalesced by imposing a flow disturbance on the bubble swarm by using a horizontal disk with a single central axial opening (rupture disk or contraction disk). The gas-in-liquid dispersion passing through this contraction disk is subjected to dynamic instabilities in the form flow expansion followed by flow contraction. The flow expansion has been achieved by positioning a horizontal screen with multiple openings (guide disk or expansion disk) above the first disk and the contraction of the two-phase dispersion has been achieved by using a hollow disk with a single central axial opening (rupture disk or contraction disk) positioned above the expansion disk. The section of the reactor consisting of a screen (expansion/guide disk) positioned between two hollow disks (contraction/rupture disk) comprises of one stage. At every stage

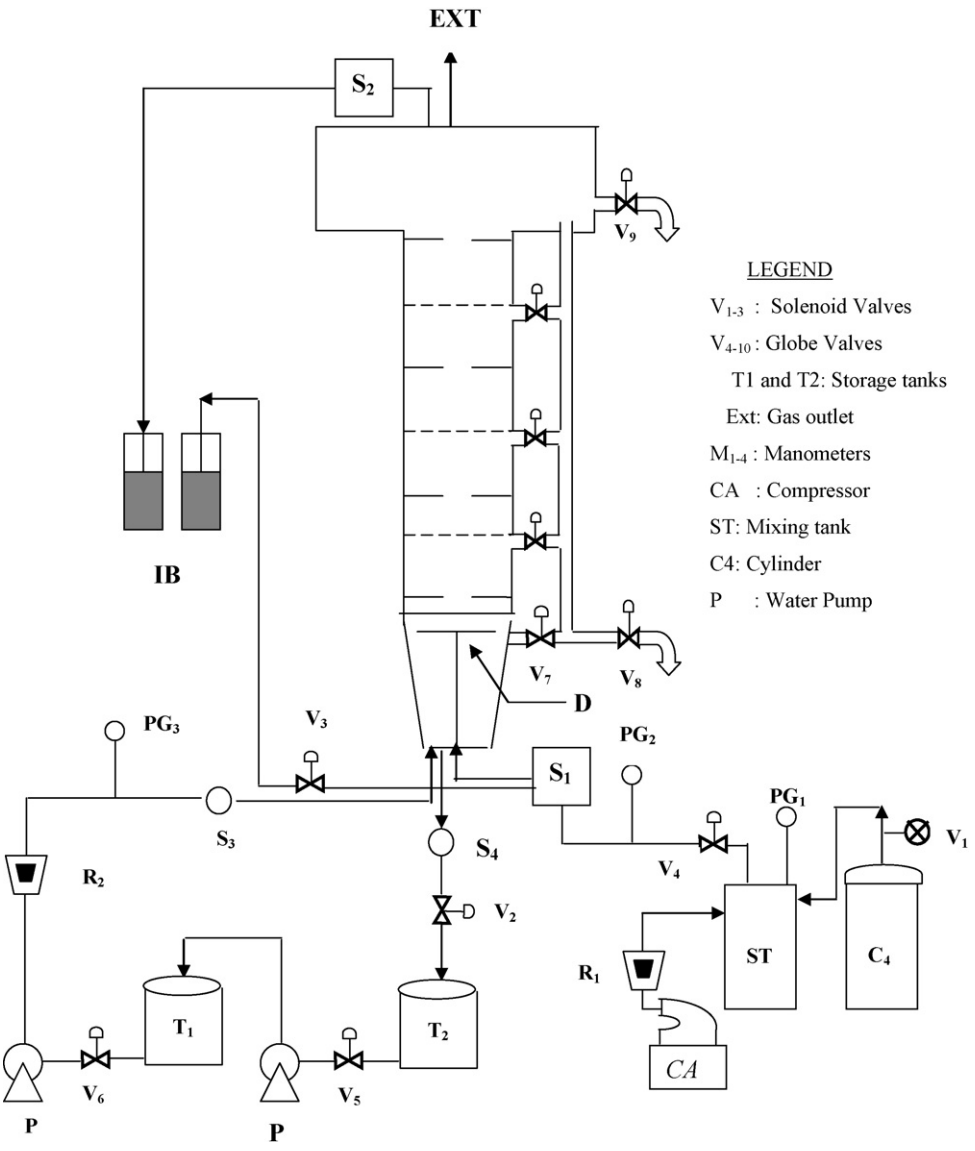

Fig. 1. Schematic diagram of the experimental setup for measuring interfacial area and mass transfer coefficient.

bubbles loose their individual identities and new bubbles are generated.

The gas hold up was determined from the two-phase pressure drop. The velocity of liquid circulation was determined with the neutral buoyancy flow follower technique. The details of the procedures and results regarding gas hold up and liquid circulation velocity is reported elsewhere [20].

In the determination of the specific interfacial area, the chemical rate of absorption of CO_2 (0.08–0.3) diluted with air in aqueous solution of sodium hydroxide (51.2–70 g mol/m^3) have been used, while sodium carbonate–bicarbonate buffer solutions were used for the measurement of liquid side mass transfer coefficient. The sodium hydroxide solutions of 1000 L capacity was prepared and stored in a holding tank T_1 for continuous operation. Outlet solution was collected in a separate tank T_2 and was recycled again to tank T_1 after proper adjustment of desired concentration. The inlet and outlet liquid samples were collected at point S_3 and S_4, respectively. Gas samples were also collected at sampling points S_1 and S_2, located at the inlet and outlet of the multi-stage external loop airlift reactor. The gas and liquid phases in the samples were continuously separated. The gas was analyzed by impingement through volumetric analysis. The liquid samples were analyzed by standard methods of titration, Vogel [21].

In actual experiments, first carbon dioxide gas obtained from pressure cylinder (C4), mixed with compressed air (CA) from laboratory supply in a mixing tank (ST). This tank was made sufficiently big so that there was undisturbed supply of constant composition of CO_2–air mixture. This mixture was fed to the bottom of the reactor along with the NaOH solutions or buffer solutions (as the case may be) in a co-current flow continuously. By controlling the individual rates of flow a constant liquid–gas dispersion volume was maintained in the reactor. After the system had attained steady state, the flow rates of the gas and liquid, the system pressure and temperature and the burette readings were noted, and the gas liquid samples were collected at the sam-

Table 1
Experimental conditions for interfacial area and mass transfer coefficient measurement

Liquid flow rate	1.66–6.66 × 10^{-4} m^3/s
Gas flow rate	3.33–13.3 × 10^{-4} m^3/s
NaOH concentration for interfacial area measurement	51.2–70 g mol/m^3
Na_2CO_3 concentration for k_La measurement	148.5–190.8 g mol/m^3
$NaHCO_3$ concentration for k_La measurement	52.3–96.5 g mol/m^3
Inlet CO_2 concentration (mol)	0.08–0.3
Diameter of the reactor (riser)	0.2199 m
Height of the reactor	1.82 m

pling points for subsequent analysis. The experimental condition for interfacial area and mass transfer coefficient measurement is shown in Table 1.

4. Results and discussions

4.1. Specific interfacial area

The experimental data of interfacial area for the present system were found to satisfy the condition for pseudo-first order reaction as given by Eq. (4). Specific interfacial area was obtained by using the Eq. (16) with knowledge of D_A, k_2 and He. The Henry's law constant, He, in ionic solution was obtained by Eq. (9). D_A, i.e. diffusivity of carbon dioxide in aqueous solution was calculated from equations suggested by Nijshing et al. [17], while k_2 was obtained from Eq. (3) proposed by Porter et al. [15]. In the experimental range of gas and liquid flows investigated, the maximum interfacial area obtained was in the order of 300 m^2/m^3.

The effect of superficial gas velocity on the specific interfacial area, a, as a function of superficial liquid velocity is shown in Fig. 2. It may be seen from the figure that interfacial area increased with increasing superficial gas velocity for a particular liquid velocity. At higher liquid velocity the system tends to generate finer bubbles, and thus increased gas holdup. This higher gas holdup results in higher interfacial area. The experimental value of gas holdup for this reactor is reported to be in the range of 0.42–0.68 [20]. The increase in gas velocity also leads to increase in gas holdup, there by increasing the interfacial area. Fig. 3 shows a typical plot of the interfacial area as a function of the liquid circulation velocity, for a constant superficial gas velocity. It can be seen from the figure that the interfacial area increased with increasing liquid circulation velocity. This may be attributed to the increase in gas holdup with increase in liquid circulation velocity.

An attempt has been made to correlate the interfacial area with the superficial gas velocity, as it was found experimentally that interfacial area is strongly dependent on the superficial gas velocity. The following equation best represent the correlation relating interfacial area with the superficial gas velocity:

$$a = 1915.13 U_G^{0.651} \quad (22)$$

Eq. (22) was obtained by multiple least square regression method. The coefficient of correlation was of the order of 0.927

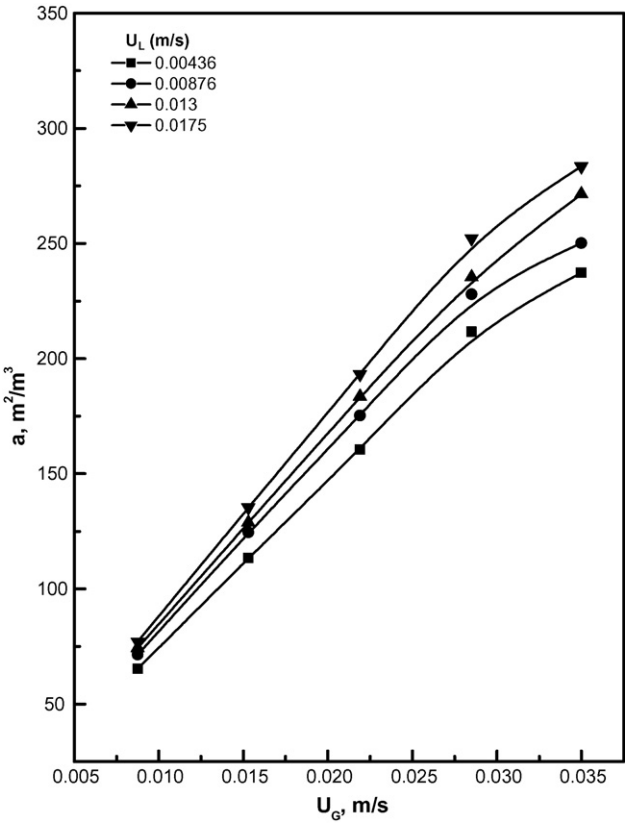

Fig. 2. Effect of superficial gas velocity on interfacial area.

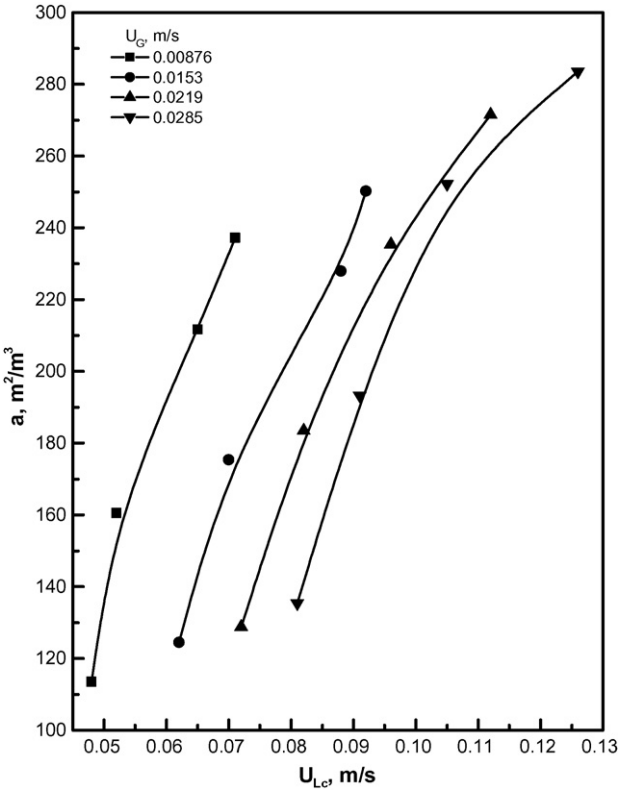

Fig. 3. Effect of liquid circulation velocity on interfacial area.

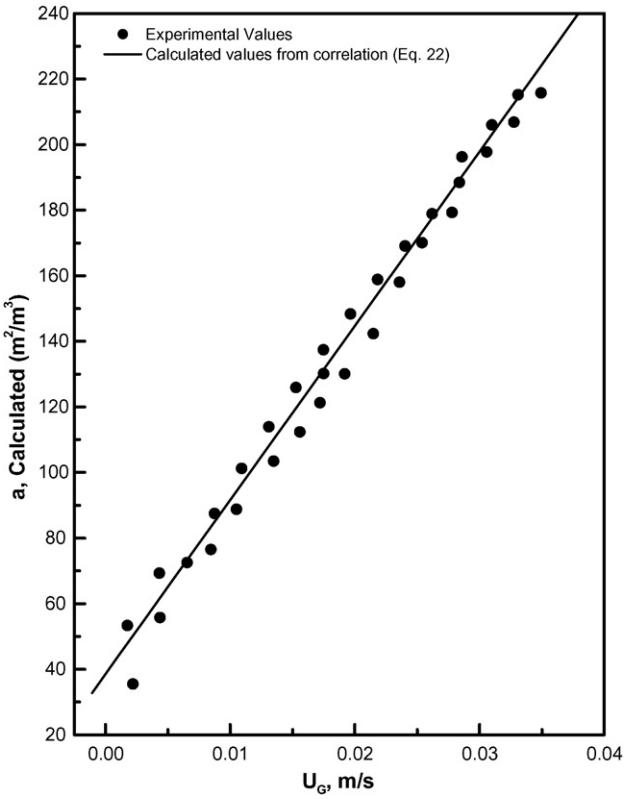

Fig. 4. Variation of interfacial area with superficial gas velocity from correlation.

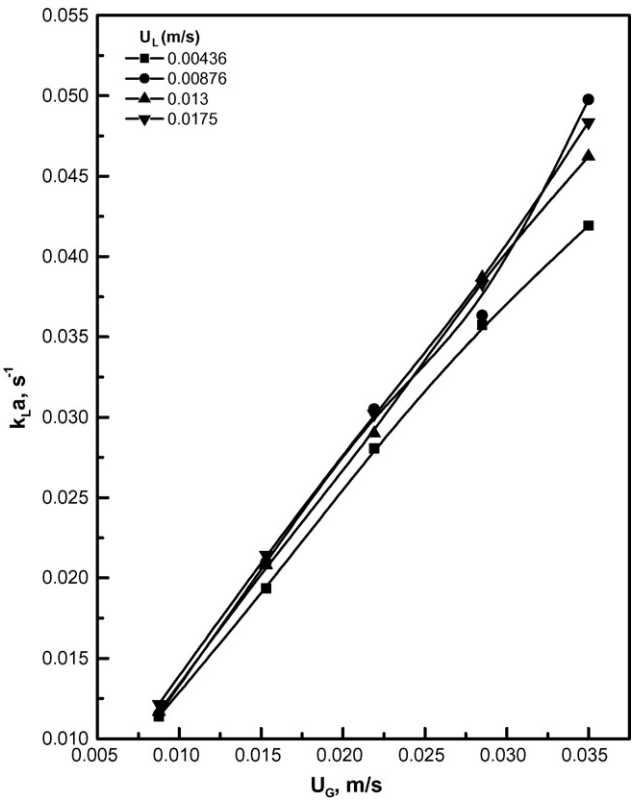

Fig. 5. Effect of superficial gas velocity on volumetric mass transfer coefficient.

and standard deviation of the experimental data from regression analysis was found to be 7.27%. The relation between the interfacial area and superficial gas velocity is shown in Fig. 4, where the solid line represents the correlation given by Eq. (22) and points are experimental values. The percentage deviation between the experimental data and those predicted by Eq. (22) has been found to be small (±4%). Thus, the empirical correlation satisfies the experimental data of the present system satisfactorily.

4.2. Liquid-side volumetric mass transfer coefficient

The liquid-side mass transfer coefficients were obtained from Eq. (21) by measuring the rate of mass transfer per unit volume and interfacial concentration of carbon dioxide. The effect of superficial gas velocity on the volumetric mass transfer coefficient as a function of superficial liquid velocity is shown in Fig. 5. It can be seen from the figures that the mass transfer coefficient increased with increasing superficial gas velocity for a particular liquid velocity. With increase in gas velocity gas holdup and turbulence of the system increases, which in turn increases the values of k_La. Fig. 6 shows a typical plot of k_La as a function of the liquid circulation velocity, for a constant superficial gas velocity. It can be seen from the figure that the volumetric mass transfer coefficient increased with increasing liquid circulation velocity, which is a result of higher mixing.

It was found experimentally that the volumetric mass transfer coefficient is strongly dependent on the superficial gas velocity. Similar types of findings were reported earlier [2,22]. Therefore,

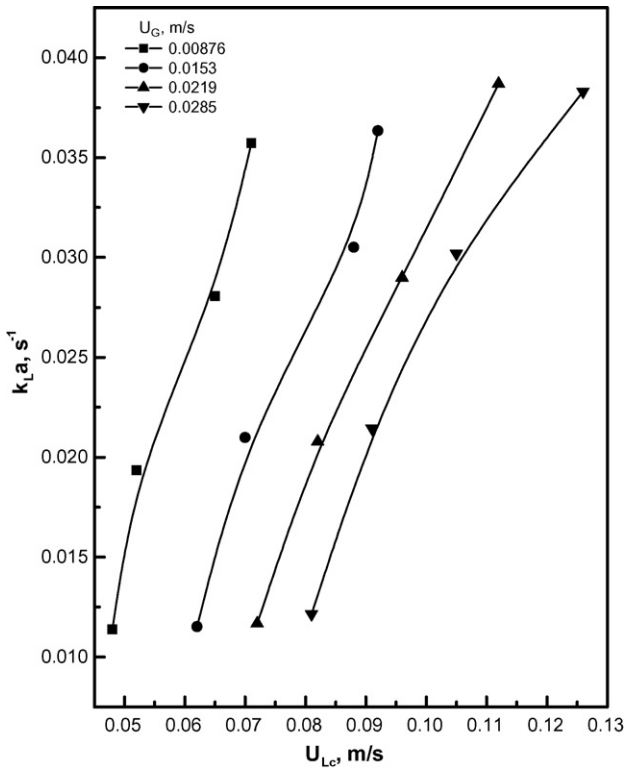

Fig. 6. Effect of liquid circulation velocity on volumetric mass transfer coefficient.

Table 2
Comparison of power consumption along with mass transfer characteristics for various gas–liquid contacting devices with the present system

Contacting equipment	Gas rate, Q_G/A_r (Nm^3/m^2 s)	Specific surface area, a (m^2/m^3)	Volumetric mass transfer coefficient, k_La (s^{-1})	Power consumption, E (W/m^3)
Plate column	0.6	100–400	0.01–0.05	1300
Packed column	0.9	200	0.005–0.02	–
Wetted wall column	2.1	50	–	–
Gas bubble column	0.02	70	0.005–0.01	400
Stirred bubble absorber	0.06	200	0.02–0.2	2600
Spray column	–	10–100	0.0007–0.015	–
Jet (loop)	–	1000–7000	0.1–3.0	10–700
Multi-stage ELALR (present work)	0.35	70–300	0.01–0.05	25–250

an attempt has been made to correlate the volumetric mass transfer coefficient with the superficial gas velocity. The following equation best represent the correlation relating volumetric mass transfer coefficient with the superficial gas velocity:

$$k_La = 0.65U_G^{0.825} \quad (23)$$

Eq. (23) was obtained by multiple least square regression method. The coefficient of correlation was of the order of 0.941 and standard deviation of the experimental data from regression analysis was found to be 4.19%. To check the consistency of the experimental data, the values of volumetric mass transfer coefficient calculated from Eq. (23) have been plotted against the experimental values in Fig. 7, where the solid line represent the regression equation and points are experimental values. The percentage deviation between the experimental data and those predicted by Eq. (23) has been found to be small (±8%). Thus, the empirical correlation satisfies the experimental data of the present system satisfactorily.

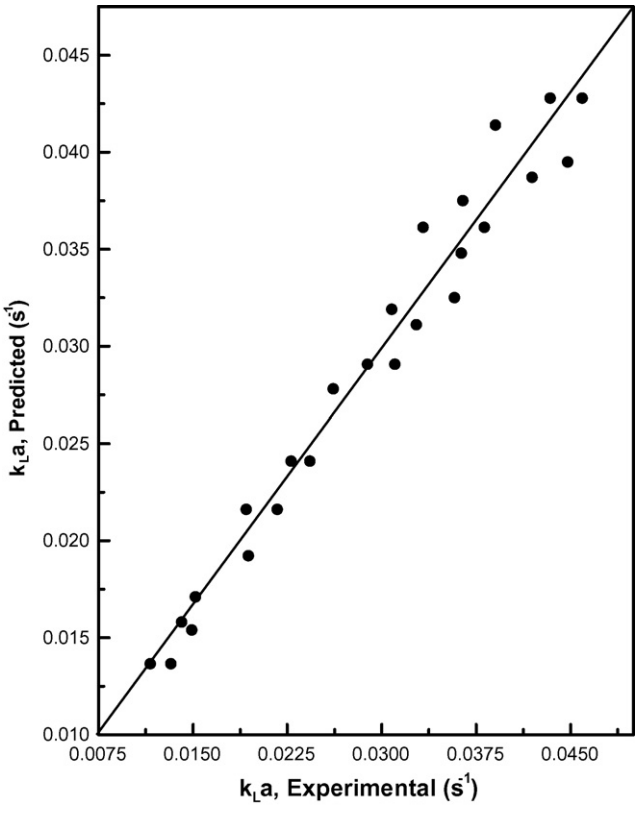

Fig. 7. Comparison of experimental values of volumetric mass transfer coefficient with that predicted from the correlation.

The power consumption, interfacial area and volumetric mass transfer coefficient of the present system have been compared with those of the other contactors and are shown in Table 2. It is interesting to note that the present system gives higher interfacial area and volumetric mass transfer coefficient with comparable power consumption.

5. Conclusions

In the present investigation a multi-stage external loop airlift reactor with hydrodynamically induced continuous bubble generation, breakup and regeneration was conceived, fabricated and characterized. The system was designed to operate with relatively large sized bubbles so that internal circulation can be induced in the liquid–bubble interfaces and faster transfer of components can take place both by turbulent diffusion through the interface of the bubbles and also due to the direct rupture of the relatively large sized bubbles. A detailed study of the interfacial area and volumetric mass transfer coefficient has been reported. The effect of superficial gas and liquid circulation velocity on a and k_La were studied. It was found experimentally that values of a and k_La are strong functions of superficial gas velocity. Thus two simple correlations of a and k_La were developed as a function of superficial gas velocity, from where the values of the parameters at any given gas velocity can be predicted. In the present system a significantly higher values of a and k_La are obtained with low power consumption in comparison with other gas–liquid contactors.

Acknowledgement

Prof. M.N. Biswas thankfully acknowledges the award of the Emeritus Fellowship by AICTE, tenable at Government College of Engineering and Leather Technology, Salt Lake, Kolkata.

References

[1] J.C. Merchuk, S. Yehuda, Local holdup and liquid velocity in airlift reactors, AIChE J. 27 (1981) 377–388.
[2] K. Choi, W.K. Lee, Circulation liquid velocity, gas holdup and volumetric oxygen transfer coefficient in external-loop airlift reactors, J. Chem. Technol. Biotechnol. 56 (1993) 51–58.

[3] Ch. Bentifraouine, C. Xuereb, J.P. Riba, An experimental study of the hydrodynamic characteristics of external loop airlift contactors, J. Chem. Technol. Biotechnol. 69 (1997) 345–349.
[4] K. Akita, F. Yoshida, Gas holdup and volumetric mass transfer coefficient in bubble columns, Ind. Eng. Chem. Process Des. Dev. 12 (1973) 76.
[5] W.D. Deckwer, Bubble Column Reactor, John Wiley & Sons, New York, 1992.
[6] M.Y. Chisti, Air-lift Bioreactors, Elsevier Applied Science, London, 1989.
[7] Y. Kawase, M. Moo-Young, Turbulence intensity in bubble columns, Chem. Eng. J. 40 (1989) 55–58.
[8] B.C. Meikap, G. Kundu, M.N. Biswas, Prediction of interfacial area of contact in a variable area multi-stage bubble column, Ind. Eng. Chem. Res. 40 (2001) 6194–6200.
[9] P.H. Calderbank, Physical rate processes in industrial fermentation. Part I. The interfacial area in gas–liquid contacting with mechanical agitation, Trans. Inst. Chem. Eng. (London) 36 (1958) 443–463.
[10] J.L. York, H.E. Stubbs, Photographic analysis of sprays, Trans. ASME 74 (1952) 1157–1161.
[11] K.D. Copper, G.F. Hewitt, B. Pinchin, Photographic method to measure interfacial area in liquid and gas dispersed system, J. Photo. Sci. 12 (1964) 269–273.
[12] M.M. Sharma, P.V. Danckwerts, Chemical methods of measuring interfacial areas and mass transfer coefficients in two fluid systems, Br. Chem. Eng. 15 (1970) 522–528.
[13] A. Mandal, G. Kundu, D. Mukherjee, Interfacial area and liquid-side volumetric mass transfer coefficient in a downflow bubble column, Can. J. Chem. Eng. 81 (2003) 212–219.
[14] P.L.T. Brian, Gas absorption accompanied by an irreversible reaction of general order, AIChE J. 10 (1964) 5.
[15] K.E. Porter, M.B. King, K.C. Varshney, Interfacial areas and liquid-film mass transfer co-efficients of a 3 ft diameter bubble cap plate derived from absorption rates of CO_2 into water and caustic soda solution, Trans. Inst. Chem. Eng. (London) 44 (1966) T274–T278.
[16] P.V. Danckwerts, Gas–Liquid Reactions, McGraw-Hill, New York, 1970, pp. 17–20 and 97–205.
[17] R.A.T.O. Nijsing, R.H. Hendriksz, H. Kramers, Absorption of CO_2 in jets and falling films of electrolyte solutions with and without chemical reaction, Chem. Eng. Sci. 10 (1959) 88–104.
[18] R.D. Voyer, A.I. Miller, Improved gas–liquid contacting in co-current flow, Can. J. Chem. Eng. 46 (1968) 335–343.
[19] H.S. Harned, B.B. Owen, The Physical Chemistry of Electrolyte Solutions, Reinhold Publishing Co., New York, 1958.
[20] K. Mohanty, D. Das, M.N. Biswas, Hydrodynamics of a novel multi-stage external loop airlift reactor, Chem. Eng. Sci. 61 (2006) 4617–4624.
[21] A.I. Vogel, Quantitative Inorganic Analysis, Longman Green, London, 1955.
[22] K. Shimizu, S. Takada, T. Takasahi, Y. Kawase, Phenomenological simulation model for gas hold-ups and volumetric mass transfer coefficients in external-loop airlift reactors, Chem. Eng. J. 84 (2001) 599–603.